Phytochemical analysis and green synthesis of silver nanoparticles using *Clerodendrum infortunatum* L. for potential antibacterial applications

Saraswati Karn[*], Akash Budha Magar[*], Ishwor Pathak[**] and Khaga Raj Sharma[*]

[*]Central Department of Chemistry, Tribhuvan University, Kirtipur, Kathmandu, Nepal.

[**]Department of Chemistry, Amrit Campus, Tribhuvan University, Kathmandu, Nepal.

Abstract: *Clerodendrum infortunatum* L. is a traditional medicinal plant used to treat various illnesses since ancient times by traditional healers of the Terai region of Nepal. The present study performed qualitative and quantitative phytochemical analysis and investigation of the antioxidant and antibacterial activities of five different solvent extracts of root, stem, and leaf. In addition, silver nanoparticles were synthesized using root aqueous extract of the plant. The methanolic extract of root contained the highest TPC and TFC values of 26.18±3.83 mg GAE/g and 7.2±1.2 mg QE/g respectively. The methanolic extract of the leaf also showed the highest DPPH radical scavenging activity with an IC_{50} of 59.96 µg/mL. In the antibacterial assay, the aqueous extract of leaf and stem showed strong antibacterial properties against *Escherichia coli* with ZOI values of 19 mm and 18 mm respectively which was more than the ZOI value of the positive control neomycin (16 mm). The aqueous root extract was successfully used in the green synthesis of silver nanoparticles. The synthesized silver nanoparticle displayed an SPR peak at 407 nm. The average diameter of nanoparticles was calculated as 11.82 nm using the Debye-Scherer equation. They were characterized using different spectroscopic techniques. Synthesized nanoparticles showed comparatively more activity against gram-negative *Klebsiella pneumoniae* than gram-positive *Staphylococcus aureus*. In conclusion, the plant is rich in phytochemicals with potent antibacterial activity. It can be effectively used in the green synthesis of nanoparticles.

Keywords: Antimicrobial; Antioxidant; *Clerodendrum infortunatum*; Green synthesis; Nanoparticles; Phytochemicals.

Introduction

Although Nepal occupies only 0.03% of the world's land area, it has a disproportionately rich biodiversity of plants and animals. Since ancient times, medicinal plants have been identified and employed in conventional medical procedures and treatments. Traditional treatment methods employing plants and their derivatives have gained international attention in recent decades. A sizable section linked to the prevention and /or management of various medical conditions as well as chronic diseases like cancer, diabetes, heart disease, and hypertension [1]. Growing rates of drug-resistant infections of clinical and agricultural significance have led to scientists looking for novel antibacterial compounds in plants[2].In vitro studies have verified the antibacterial qualities of flavonoids, terpenoids, tannins, and alkaloids [3].

Nanomaterials are substances that have dimensions in the nanoscale range. The astonishing properties of nanoparticles have led to the development of several innovative uses in the pharmaceutical, medical, electronics, agricultural, chemical catalysis, food, and many other disciplines [4]. There are different physical and

Author for correspondence : Khaga Raj Sharma, Central Department of Chemistry, Tribhuvan University, Kirtipur, Kathmandu, Nepal.
Email: khaga.sharma@cdc.tu.edu.np ; https://orcid.org/0000-0002-1555-0887
Received: 5 Jan, 2025; Received in revised form: 14 Feb, 2025; Accepted: 1 April, 2025.
Doi: https://doi.org/10.3126/sw.v18i18.78515

chemical techniques for synthesizing nanoparticles.

Green synthesis is highly preferred due to its environment-friendly nature. Silver nanoparticles (Ag NPs) have been extensively studied due to their wide applications in water purifications,medical devices, and home disinfectants [5]. They are recognized as a superior antibacterial agent that can combat multidrug-resistant bacteria [6]. The unique properties of silver nanoparticles can be incorporated into the fields of food packaging, cosmetics, bioengineering, electrochemistry, catalysis, and antiseptic agents in the medical industry [7].

C. infortunatum Linn. (Family: Verbanaceae), locally known as Bhant, is a terrestrial shrub. In traditional medicine, it is used to treat bronchitis, asthma, fever, burning sensations, blood diseases, inflammation, and epilepsy. The plant is reported for potent antimicrobial properties[8]. So, the present study involved the synthesis of silver nanoparticles from the aqueous extract of this plant and the investigation of the antimicrobial properties, which has not been well reported in the literature. In addition, the study evaluated the total phenolic content, the total flavonoid content, antioxidant potential, and a comparative study of the antimicrobial properties of various crude extracts in different solvents**.**

Figure 1: Flowers and leaves of Clerodendrum infortunatum Linn. (left) and plant in its natural habitat (right).

Methods and Methodology

Sample collection and identification

The sample of the plant *C. infortunatum* L. was collected in its natural habitat from Mahendranagar, Chhireshwarnath Municipality of the Dhanusa District, Nepal in October and November 2022. The plant was identified by the National Herbarium and Plant Laboratories, Godawari, Kathmandu with an identification number of SK01. The photograph of the plant sample from the collection site is provided in Figure 1.

Sample preparation

The leaves, stems, and roots of the collected plant sample were separated thoroughly washed with water, dried in the shade for almost two weeks, crushed into powder, and stored in individual zip-lock plastic bags. Then five different solvents with increasing order of polarity (hexane, ethyl acetate, dichloromethane, methanol, and water) were used to prepare solvent extracts of plant parts. About 30g of the sample powder (leaf, stem, and root) was taken in a conical flask and 300 mL of extraction solvent (hexane, ethyl acetate, dichloromethane, methanol, or water) was added. The flask was thoroughly shaken every 24 hours. After 72 hours, the contents in the flask were filtered and the filtrate was concentrated in a rotary evaporator to obtain crude extracts. The yield % of the crude extract was determined using the following formula:
Yield percentage = Weight of dried crude extract/ Weight of sample * 100.

Phytochemical analysis

C. infortunatum L. solvent extracts were subjected to qualitative phytochemical analysis. The screening procedure followed standard protocols with slight modifications[9].

Total phenolic content (TPC)

Using the Folin-Ciocalteu reagent with gallic acid as the standard, the total phenolic contents in different solvent extracts of the leaf, stem, and root *Clerodendrum infortunatum* L. were evaluated based on an oxidation-reduction reaction[10]. 20 µL each of gallic acid solutions at different concentrations and plant extract solutions (5 mg/mL) were added to the bores of a 96-well plate. Then, each well received 100 µL of FCR reagent (1:10 in distilled water) and 80 µL of 1 M sodium carbonate solution. The plate was incubated in the dark for 25

minutes and absorbance was measured at 760 nm. Finally, TPC was calculated using a gallic acid calibration curve and expressed in terms of mg GAE/g.

Total flavonoid content (TFC)

Total flavonoid content was measured with the help of the $AlCl_3$ colorimetric method with slight adjustments [11]. 20 µL of 5 mg/mL plant extract, 110 µL of distilled water, .60 µL of ethanol, 5 µL of 1 M $AlCl_3$, and 5 µL of 1 M CH_3COOK were added to the bores of 96-well plate. In some bores, the volume of distilled water and plant extract solutions was replaced with 130 µL of standard quercetin solutions at different concentrations. The plate was incubated for 30 minutes in the dark and absorbance was measured at 415 nm with the help of a well plate reader. TFC was measured from the standard quercetin calibration curve and expressed in terms of mg QE/g.

Antioxidant activity

The antioxidant activity in plant extracts was measured using the DPPH (1,1-diphenyl-2-picrylhydrazil) assay [12]. 100 µL of 0.1 mM DPPH (in ethanol) and 100 µL of plant extracts at different concentrations were mixed inside the bores of a 96-well plate. The plate was placed in the dark for 30 minutes and absorbance was recorded at 517 nm. Quercetin and 50% DMSO acted as positive and negative controls, respectively.

The % of the DPPH free radical inhibition was determined as:

$$\%\text{Inhibition} = (A_O - A_S)/ A_O * 100$$

Where, A_O= absorbance of the control (DPPH solution + methanol) and A_S=absorbance of the test sample.

The effective concentration of the sample needed to scavenge 50% of the DPPH free radicals is represented by the IC_{50} (50% inhibitory concentration). It was calculated from the percentage inhibition versus concentration curve.

Antimicrobial screening

The antimicrobial activities of plant extracts were analyzed using the agar-well diffusion method[13]. Bacterial inoculum (0.5 McFarland standard) prepared in growth media was spread onto Muller Hinton Agar plates. Aliquots of 50 µL plant extract solutions (25 mg/mL) were added to the wells (6 mm diameter) prepared in the MHA plates and the plates were incubated for 24 hours at 37 °C. The next day, zones of inhibition were measured with the help of a ruler. Neomycin and 50% DMSO acted as positive control and negative control respectively.

Synthesis of silver nanoparticles

The standard protocol was followed for the synthesis of silver nanoparticles[14]. Firstly, a finely powdered root sample (20 g) of *C. infortunatum* L. was added to 400 mL of distilled water and heated for 15 to 20 minutes at 60 °C on a magnetic hot plate stirrer. The mixture was cooled and filtered to obtain an aqueous extract [15].

The aqueous extract was reacted with 1 mM silver nitrate in ratios of 1:9 (10 mL extract and 90 mL $AgNO_3$ solution), 1:4 (20 mL extract and 80 mL $AgNO_3$ solution), and 1:1 (50 mL extract and 50 mL $AgNO_3$ solution). The ratio of 1:9 was found to be ideal for producing silver nanoparticles. The synthesis of silver nanoparticles was attempted using the aqueous extracts of root, stem, and leaf. However, the stem and leaf extracts did not show considerable peaks in the 300-600 nm scanning range of UV spectroscopy. So, they were discarded. The root aqueous extract was chosen for further steps as it showed stable and distinct peaks in UV-visible spectroscopy.

Thus, 50 mL of root extract and 450 mL of the 1 mM $AgNO_3$ solution were reacted, and the liquid mixture was constantly agitated at room temperature for nearly 30 minutes on a magnetic hot plate stirrer. The color shift of the reaction mixture from light yellow or brown to strong brown indicated the formation of silver nanoparticles in the solution.

Characterization of silver nanoparticles

The characterization of the nanoparticles was done to evaluate the size, shape, homogeneity, dispersity, and morphological conformance using a range of techniques after synthesis. UV-Visible Spectroscopy, X-Ray Diffraction (XRD), Fourier-transform infrared spectroscopy (FTIR), Field – emission Electron Microscopy (FE-SEM), and Energy Dispersive X-ray

Analysis (EDAX) are the methods used to characterize the nanoparticles.

Antibacterial activity of silver nanoparticles

The antibacterial activity of synthesized silver nanoparticles from the root aqueous extract of *C. infortunatum* L. was evaluated using the disc diffusion method[16]. Paper discs with diameters of around 6 mm were made using a punching machine and Whatman filter paper and autoclaved. Nanoparticle suspension was prepared by sonicating 50 mL of nanoparticle solution in 1000 mL of deionized water (1:20 v/v) for 30 minutes. The sterile discs were then dipped into the nanoparticle suspension using a sterile tong and left to dry in the laminar hood. Neomycin acted as the positive control, while deionized water acted as the negative control.

Results and Discussion

Percentage yield

The percentage yields of different solvent extracts are presented in Figure 2. The values were higher in more polar solvents like water and methanol. Similarly, Root extract showed the highest percentage yield, followed by leaf and stem.

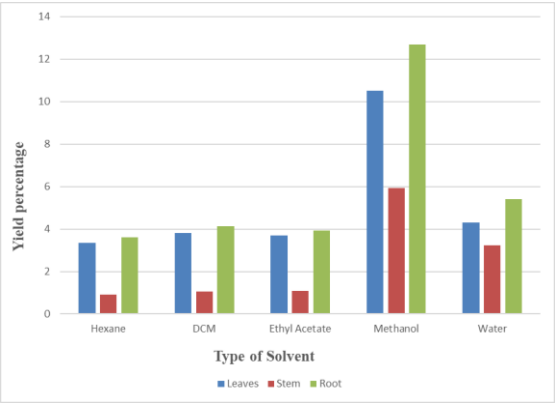

Figure 2: Percentage yield for different solvent extracts.

Qualitative phytochemical screening

The result of phytochemical screening is presented in Table 1. Polyphenols, flavonoids, tannins, and alkaloids were detected in methanol extracts of *C. infortunatum* L. These phytochemicals play a crucial role as capping and reducing agents in the synthesis of silver nanoparticles. They are responsible for the biological activities and medicinal properties of the plant.

Total phenolic content

The methanolic extract of root showed the highest TPC (26.18 ± 3.83 mg GAE/g), which gives the methanolic extract its strong antioxidant potential[17]. It was followed by ethyl acetate extract from the stem (23.82 ± 1.26mg-GAE/g) and methanol extract from the leaf (22.28 ± 1.76 mg GAE/g). The least amounts of phenolic contents were recorded for hexane extracts whereas methanol extracts showed the highest values. This is caused due to the polar nature of phenolic compounds that are easily extracted by polar solvent (methanol)[18]. Among different parts of the plant, root extract showed the highest phenolic concentration followed by the leaf and stem. TPC values of different plant extracts are presented in Figure 3.

Table 1: Qualitative phytochemical analysis of methanol extracts of *Clerodendrum infortunatum* L.

Phytochemicals	methanol extracts of		
	Leaf	Stem	Root
Tannins	+	+	+
Flavonoids	+	+	+
Phenolic compounds	+	+	+
Carbohydrates	-	+	+
Alkaloids	+	+	+

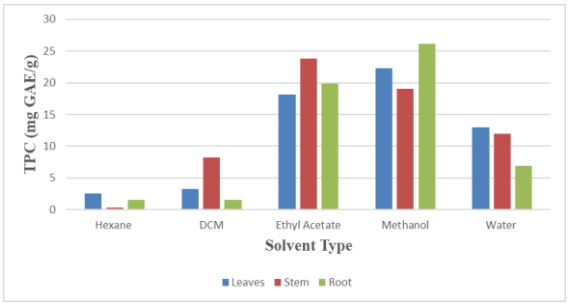

Figure 3: Total phenolic content in different solvent extracts.

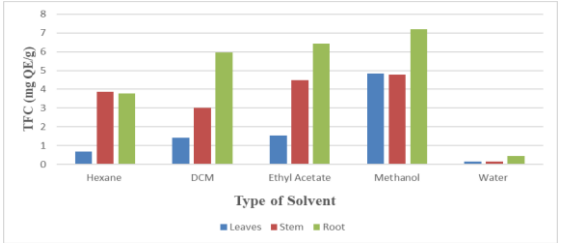

Figure 4: Total flavonoid content in different solvent extracts.

Total flavonoid content (TFC)

The methanol extract of roots contained the highest amount of TFC (7.20±1.20 mg QE/g). The ethyl acetate extract of root followed in second, with a TFC value of 6.43±1.54 mg QE/g, whereas the leaf aqueous extract had the lowest TFC value, measuring only 0.14±0.09 mg QE/g. The total flavonoid content varied in different parts of the plant and different solvent extracts. Polar methanol solvent extracts contained the highest concentrations of flavonoids, whereas hexane extracts recorded the lowest ones. Even though flavonoids are polar compounds, small concentrations of flavonoids recorded in hexane and ethyl acetate may be due to the presence of O-methylated non-polar flavonoid compounds. Similarly, TFC was the maximum in root extracts. The TFC for different extracts is graphically presented in Figure 4.

Antioxidant activity

The extracts of *C. infortunatum* L. showed considerable antioxidant activities (Figure 5). Methanol leaf extract displayed an IC_{50} value of 59.96 µg/mL, whereas IC_{50} values of 341.29 and 372.86 µg/mL, respectively were recorded for hexane and DCM extracts.

For stem extracts, ethyl acetate and methanol extracts had good antioxidant potential with IC_{50} of 60.09 and 75.19 µg/mL, respectively, while DCM extract showed moderate antioxidant activity with an IC_{50} of 360.211 µg/mL. For the root extracts, the ethyl acetate extract showed strong antioxidant activity (IC_{50}: 72.23 µg/mL), while the potential was weaker in the hexane extract (IC_{50}: 361.44 µg/mL). On the other hand, the DCM and methanolic extracts of roots with IC_{50} of 234.58 and 163.41 µg/mL, respectively, demonstrated moderate antioxidant activity. Thus, ethyl acetate extracts from the stem and methanolic extracts from the leaves can be used as natural antioxidants. However, the IC_{50} values were higher compared to 2.34 µg/mL recorded for standard quercetin.

Antimicrobial activity

Aqueous extract of the leaf and stem of *C. infortunatum* L. showed excellent antibacterial activity against *Escherichia coli* ATCC-25922 with ZOI of 19 mm and 18 mm respectively. These values were higher than the ZOI of the positive control neomycin (16 mm). Similarly, the ZOI of 24 mm for aqueous extract of leaf against *Shigella sonnei* ATCC-25931 equaled the ZOI of neomycin (24 mm). No zone of inhibition was formed in the methanolic extract of

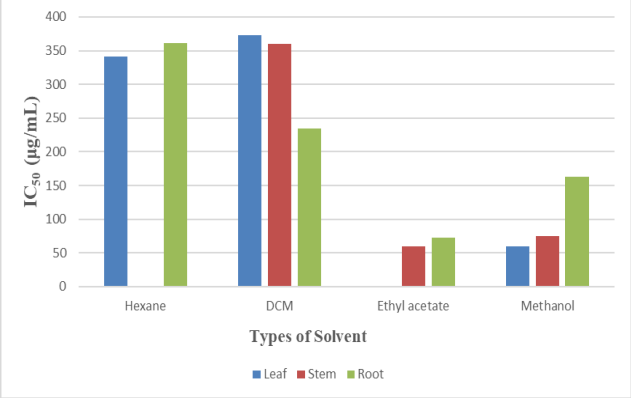

Figiure 5: Free radical scavenging activity in different solvent extracts.

the leaf against *Escherichia coli* ATCC-25922 and hexane extract of root against *Klebsiella pneumonia*ATCC-700603. Among all extracts, aqueous extracts showed comparatively higher antibacterial properties. The extracts of *C. infortunatum* L. showed higher activity towards gram-positive bacteria compared to gram-negative bacteria. The ZOI of different plant extracts against selected bacteria strains are presented in Figures 6 to 8. Similarly, Figures 9 to 12 present photographs of Petri plates taken during the antibacterial assay.

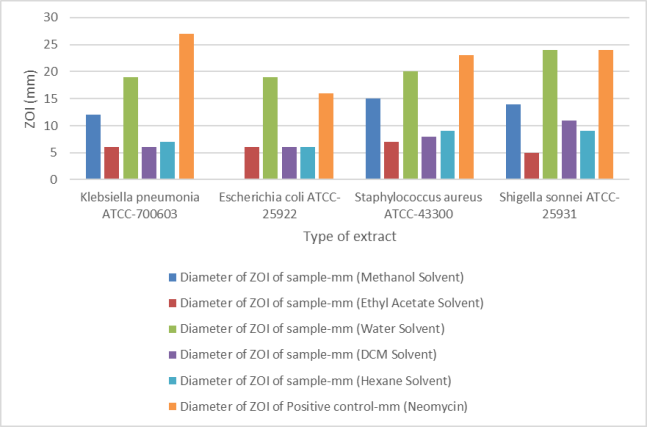

Figure 6: ZOI of various leaf extracts against selected bacteria.

Characterization of silver nanoparticles

A 1:9 solution mixture of root aqueous extract of *C.*

infortunatum L. and 1 mM of aqueous $AgNO_3$ solution maintained within a pH range of 11 to 13 started to develop a reddish-brown color after twenty-four hours. The color shift of the solution indicated the formation of silver nanoparticles in the solution. The UV-visible spectroscopic analysis confirmed the production of silver nanoparticles.

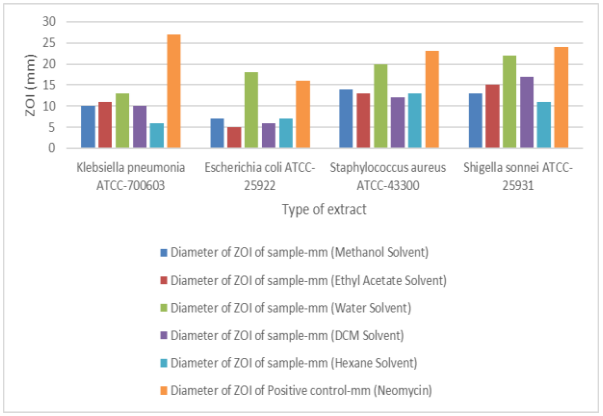

Figure7: ZOI shown by stem extracts against selected bacteria.

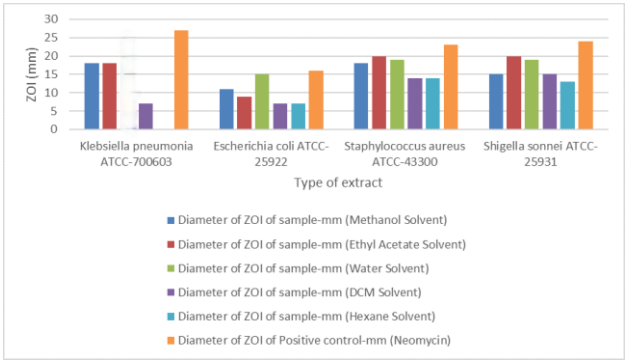

Figure 8: **ZOI shown by root extracts against selected bacteria.**

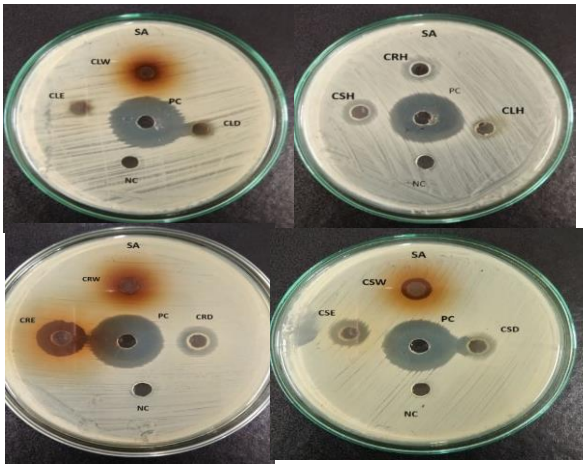

Figure 9: Photographs of Petri plates showing ZOI of plant extracts against *Staphylococcus aureus*. (C; *Clerodendrum*, R; root, S; stem, L; leaf; W; water, M; methanol, D; dichloromethane, E; ethyl acetate, and H; hexane extracts).

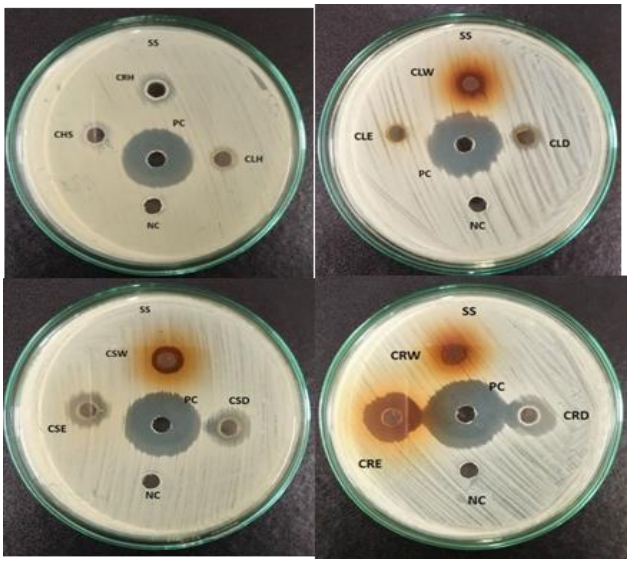

Figure 10: Photographs of Petri plates showing ZOI of plant extracts against *Shigella sonnei pneumonia.*

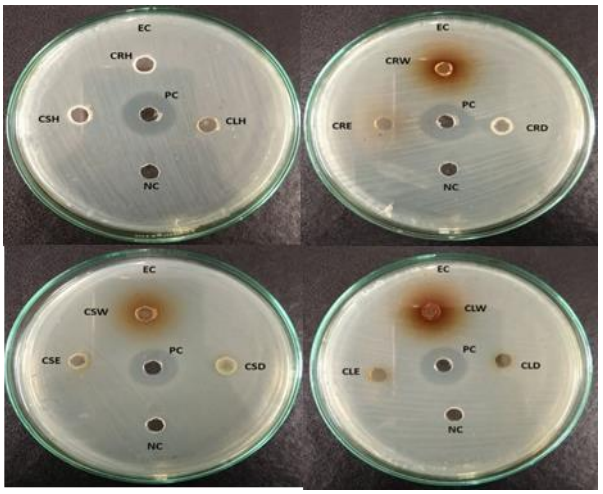

Figure 11: Photographs of Petri plates showing ZOI of plant extracts against *Escherichia coli.*

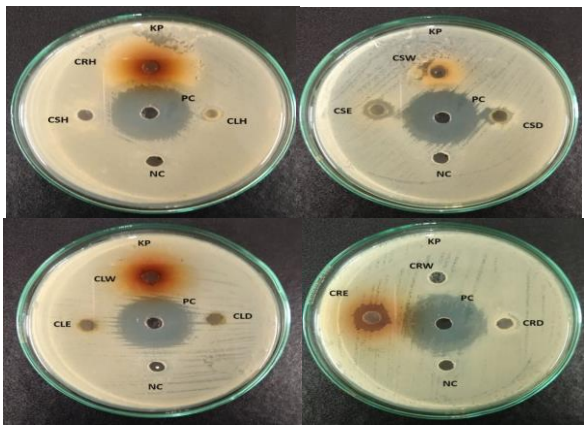

Figure 12: Photographs of Petri plates showing ZOI of plant extracts against *Klebsiella pneumoniae*.

UV – UV-visible spectroscopy

The synthesized silver nanoparticles were examined

through the UV-visible spectrophotometer within 300 to 600 nm wavelength. A Surface Plasmon Resonance (SPR) absorption band appearing in metal nanoparticles was used to confirm their formation. The UV-visible spectra of synthesized silver nanoparticles showed an absorption maxima at 407 nm (Figure 13) which is similar to 421 and 409 nm reported for silver nanoparticles synthesized using *Polystichum lentum* and *Persicaria perfoliata* aqueous exztracts[19, 20].

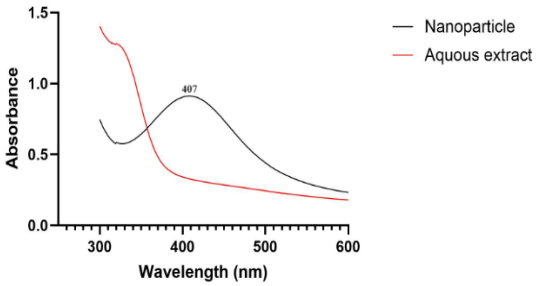

Figure 13: UV-vis Spectral analysis of synthesized nanoparticles using root extract.

Fourier transfer infrared spectroscopy (FTIR)

FTIR analysis within a wavelength range of 400-4000 cm^{-1} was performed to study organic functional groups adsorbed on the surface of the nanoparticles, biomolecule bonding information, and the fraction of H-bonding. FTIR spectra of dried silver nanoparticles and aqueous root extract were recorded and presented in Figure 14. The FTIR spectrum of plant extract displayed a peak at 3255 cm^{-1} corresponding to the -OH bond. This peak has shifted to 3286 cm^{-1} in the silver nanoparticles. This increase in frequency is caused by the loss of hydrogen bonding and the interaction of hydroxyl groups with silver nanoparticles. Similarly, aromatic -C-H stretching frequency has shifted from 2929 cm^{-1} in aqueous extract to 2922 cm^{-1} in nanoparticles. The peaks at 1602, 1411, and 1033 cm^{-1} in aqueous extract represent C=C-stretching, -C-O stretching, and -C-N- bending. These peaks have shifted to 1600, 1409, and 1055 cm^{-1} in silver nanoparticles. These shifts in vibration frequencies are caused by the interactions of plant secondary metabolites with silver nanoparticles.

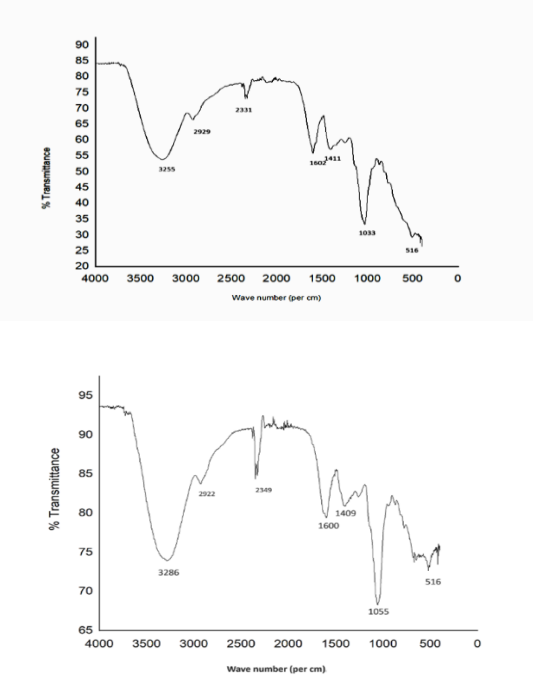

Figure 14: FTIR spectral analysis of aqueous extract of root (top) and synthesized silver nanoparticles (bottom).

X-ray diffraction (XRD)

The crystallite properties of synthesized silver nanoparticles were examined through X-ray diffraction. The XRD pattern presented in Figure 15 shows peaks at 38.25°, 44.43°, 64.60°, and 77.46°. These peaks correspond with Miller indices of (111), (200), (220), and (311) of a face-centered cubic crystal. FCC structure for the green synthesized nanoparticles that is also reported in previous literature[19, 20]. The average crystalline size of the silver nanoparticles was calculated as 11.82 nm with the help of Debye Scherrer's equation.

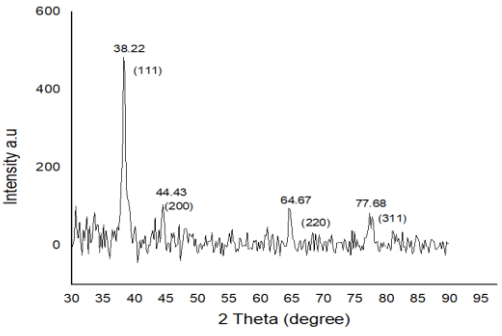

Figure 15: XRD pattern of synthesized nanoparticles using the root aqueous extract.

Field emission scanning electron microscopy (FE-SEM)

The surface morphology of the produced nanoparticles was analyzed using Field Emission Scanning Electron

Microscopy (FE-SEM). The FE-SEM images of nanoparticles are provided in figure 16 and a histogram showing particle size distribution is provided in figure 17. The average grain size of the nanoparticles was determined to be 13.14 nm using ImageJ software. This value is smaller than previously reported grain sizes of 61.33 nm and 44.28 nm for silver nanoparticles synthesized using *Polystichum lentum* and *Persicaria perfoliata* aqueous exztracts[19, 20].

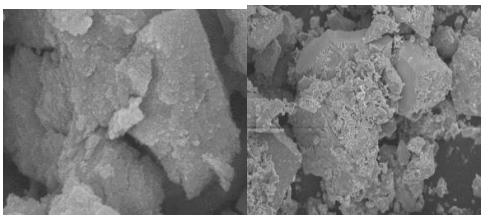

Figure 16: FE-SEM image of synthesized nanoparticles at 500 nm (left) at 50 µm (right).

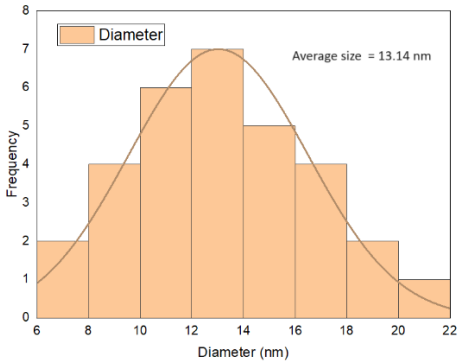

Figure 17: Distribution of particle size of synthesized nanoparticle using root extract.

Energy dispersive x-ray spectroscopy (EDX)

The EDX spectrum of synthesized nanoparticles shows a peak around 3 keV for silver. The presence of carbon, oxygen, and thorium is shown in the EDX spectrum (figure 19). Carbon and oxygen detected by EDX spectroscopy come from plant metabolites adsorbed on the surface of the nanoparticle. The elemental mapping of silver nanoparticles is shown in Figure 18.

Antimicrobial activity of AgNPs

The antibacterial activity of silver nanoparticles were measured using the disc diffusion method. Silver nanoparticles displayed ZOI of 8 mm against *Klebsiella*

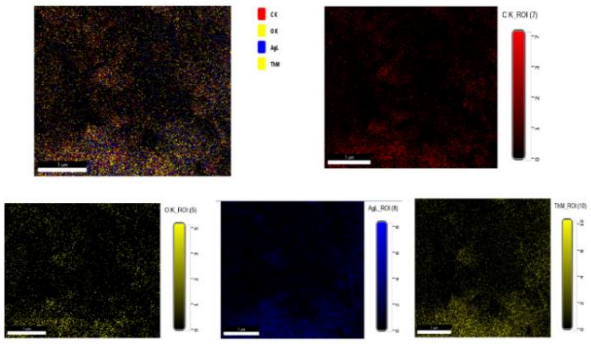

Figure 18: EDX spectra of silver nanoparticles showing total elemental mapping.

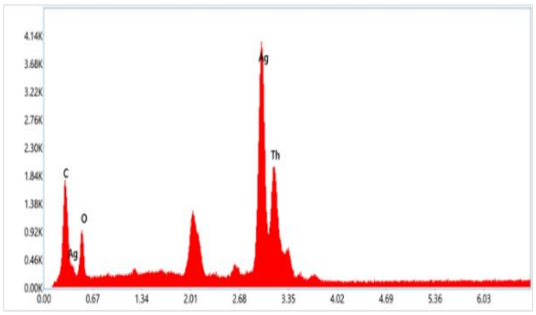

Figure 19: EDX spectra of silver nanoparticles synthesized using the root extract.

pneumoniae ATCC-700603 and 2 mm against *Staphylococcus aureus* ATCC-43300 (Figure 20). These values are significantly lower than ZOIs of 24 and 19 mm recorded for root aqueous extract of the plant in the agar well diffusion assay. The higher activity in root aqueous extract is due to the abundance of plant secondary metabolites with antibacterial properties. Positive control neomycin displayed ZOI of 22 mm against *Klebsiella pneumoniae* ATCC-700603 and ZOI of 18 mm against *Staphylococcus aureus* ATCC-43300.

The photographs of the Petri plates are provided in Figure 21.

Conclusions

C. infortunatum L. extracts showed significant phenolic and flavonoid content. They also possessed high antioxidant and antibacterial properties. Additionally, the successful synthesis of silver nanoparticles using the root aqueous extract demonstrated a green and efficient approach to nanoparticle production. The synthesized

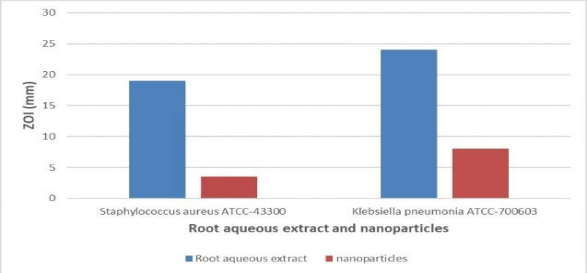

Figure 20: Antibacterial activity of silver nanoparticles against selected bacteria.

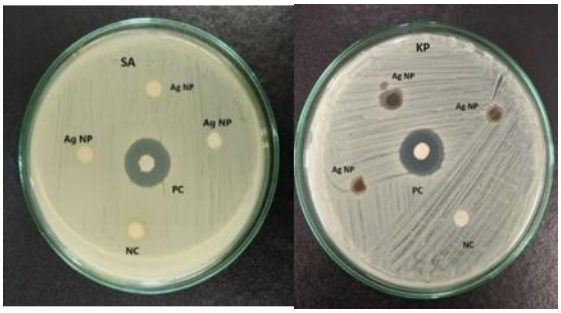

Figure 21: Photographs of petri plates showing ZOI shown by silver nanoparticles against *Staphylococcus aureus* (left) and *Klebsiella pneumoniae.* (right).

nanoparticles exhibited comparatively higher activity against gram-negative *Klebsiella pneumoniae* than gram-positive *Staphylococcus aureus*. However, the antibacterial activity in silver nanoparticles was lower than in root aqueous extract. The findings confirm *C. infortunatum* is a promising medicinal plant with applications in pharmacology and green synthesis of nanoparticles. Continued research into the pharmacological properties of the plant and its nanoparticles could lead to innovative solutions in combating bacterial resistance and advancing nanomedicine.

References

[1] Craig, W. J. 1997. Phytochemicals: Guardians of our health. *J. Am. Diet. Assoc.* **97**: S199-S204.
Doi : https://doi.org/10.1016/s0002-8223(97)00765-7

[2] Das, K., Tiwari, R. K. S. and Shrivastava, D. K. 2010. Techniques for evaluation of medicinal plant products as antimicrobial agent: Current methods and future trends. *J. Med. Plant Res.* **4**(2): 104-111.

[3] Cowan, M. M. 1999. Plant products as antimicrobial agents. *Clinical microbiology reviews.* **12**(4): 564-582.
Doi: https://doi.org/10.1128/cmr.12.4.564

[4] Joudeh, N. and Linke, D. 2022. Nanoparticle classification, physicochemical properties, characterization and applications: a comprehensive review for biologists. *Journal of Nanobiotechnology*. **20**(1): 262.
Doi: https://doi.org/10.1186/s12951-022-01477-8

[5] Yu, S. J., Yin, Y. G. and Liu, J. F. 2013. Silver nanoparticles in the environment. *Environmental Science: Process and Impacts.* **15**(1): 78–92.
Doi: https://doi.org/10.1039/c2em30595j

[6] Bruna, T., Maldonado-Bravo, F., Jara, P. and Caro, N. 2021. Silver nanoparticles and their antibacterial applications. *International journal of molecular sciences.* **22**(13): 7202.
Doi: https://doi.org/10.3390/ijms22137202

[7] Keat, C. L., Aziz, A., Eid, A. M. and Elmarzugi, N. A. 2015. Biosynthesis of nanoparticles and silver nanoparticles. *Bioresources and Bioprocessing.* **2**: 1-11
Doi : https://doi.org/10.1186/s40643-015-0076-2

[8] Waliullah, T. M., Yeasmin, A. M., Wahedul, I. M. and Parvez, H. 2014. Evaluation of antimicrobial study in *in vitro* application of *Clerodendrum infortunatum* Linn. *Asian Pacific Journal of Tropical Disease*. **4**(6): 484-488.
Doi: https://doi.org/10.1016/s2222-1808(14)60611-3

[9] Verma, R. K. and Verma, S. K. 2006. Phytochemical and termiticidal study of *Lantana camara var. aculeata* leaves. *Fitoterapia* .**77**(6): 466-468.
Doi: https://doi.org/10.1016/j.fitote.2006.05.014

[10] Tamilselvi, N., Krishnamoorthy, P., Dhamotharan, R., Arumugam, P. and Sagadevan, E. 2012. Analysis of total phenols, total tannins, and screening of phytocomponents in *Indigofera aspalathoides* (Shivanar Vembu) Vahl EX DC.*Journal of chemical and pharmaceutical research*. **4**(6): 3259-3262.
Doi: https://doi.org/10.1007/springerreference_68721

[11] Pallab, K., Tapan, B., Tapas, P. & Ramen, K. 2013. Estimation of total flavonoids content (TFC) and antioxidant activities of methanolic whole plant extract of *Biophytum sensitivum* Linn. *J. Drug Deliv. Ther.* **3**: 33-37.
Doi: https://doi.org/10.22270/jddt.v3i4.546

[12] Sutharsingh, R., Kavimani, S., Jayakar, B., Uvarani, M. and Thangathirupathi, A. 2011. Quantitative phytochemical estimation and antioxidant studies on aerial parts of *Naravelia zeylanica* dc. *International journal of pharmaceutical studies and research.* **2**(2): 52- 56.

[13] Joshi, B., Panda, S. K., Jouneghani, R. S., Liu, M., Parajuli, N., Leyssen, P., Neyts, J. and Luyten, W., 2020. Antibacterial, antifungal, antiviral and anthelmintic activities of medicinal plants of nepal selected based on ethnobotanical evidence. *Evidence-. Based Complementary and Alternative Medicine.* **2020**(1): 1043471.
Doi: https://doi.org/10.1155/2020/1043471

[14] Jalab, J., Abdelwahed, W., Kitaz, A. and Al-Kayali, R. 2021. Green synthesis of silver nanoparticles using aqueous extract of *Acacia cyanophylla* and its antibacterial activity. *Heliyon* **7**(9).
Doi: https://doi.org/10.1016/j.heliyon.2021.e08033

[15] Saratale, R. G., Saratale, G. D., Cho, S. K., Ghodake, G., Kadam, A. and Kumar, S. et. al. 2019. Phyto-fabrication of silver nanoparticles by *Acacia nilotica* leaves: Investigating their antineoplastic, free radical scavenging potential and application in H_2O_2 sensing. *Journal of the Taiwan Institute of Chemical Engineers.* **99**: 239-249.
Doi: https://doi.org/10.1016/j.jtice.2019.03.003

[16] Cunha, F. A., Maia, K. R., Mallman, E. J. J., Cunha, M. C. S. O., Maciel, A. A. M., Souza, I. P., Menezes, E. A. and Fechine, P. B. A. 2016. Silver nanoparticles-disk diffusion test against *Escherichia coli* isolates *Revista do Instituto de Medicina Tropical de São Paulo*. **58**: 73.
Doi: https://doi.org/10.1590/s1678-9946201658073

[17] Budha Magar, A., Shrestha, D., Pakka, S. and Sharma, K. R. 2023. Phytochemistry, biological, and toxicity study on aqueous and methanol extracts of *Chromolaena odorata*. *Science World Journal*. **2023**: 6689271.
Doi: https://doi.org/10.1155/2023/6689271

[18] Bhusal, M., Sharma, K., Magar, A. B., Pant, J. and Sharma, K. R. 2024. Chemical analysis and biological activities on solvent extracts from different parts of *Rhus chinensis* mill. *Natural Product Research.* **1**-7.
Doi: https://doi.org/10.1080/14786419.2024.2387831

[19] Shrestha, D. K., Magar, A. B ., Bhusal, M., Baraili, R., Pathak, I., Joshi, P. R., Parajuli, N. and Sharma, K. R. 2024. Synthesis of silver and zinc oxide nanoparticles using *Polystichum lentum* extract for the potential antibacterial, antioxidant, and anticancer activities. *Journal of Chemistry*. **2024**: 18765060.
Doi: https://doi.org/10.1155/2024/1876560

[20] Shrestha, D. K., Jaishi, D. R., Ojha, I., Ojha, D. R., Pathak, I., Magar, A. B., Parajuli, N. and Sharma, K. R. 2024. Plant-assisted synthesis of silver nanoparticles using *Persicaria perfoliata* (L.) for antioxidant, antibacterial, and anticancer properties. *Heliyon.* **10**(23).
Doi: https://doi.org/10.1016/j.heliyon.2024.e40543